Quantifying city dynamics: exploring the urban features representation of Milan's streets

Gabriele Stancato

Abstract

This study focuses on measuring, analyzing and representing the spatial distribution and correlations between urban visual features in Milan, Italy, within the context of the Multilayered Urban Sustainability Action (MUSA) project. Using Geographic Information System, Google Street View, and deep learning technologies, the research systematically analyzes streetlevel panorama pictures generated at sparse points in the city. Images are segmented according to urban categories ADE20K, focusing on greenery, ground, buildings, and sky. Through spatial continuity analysis, variograms reveal an anisotropic pattern, indicating significant visual continuity on specific orientations. The study discusses relationships among urban features, such as the inverse proportionality between greenery and buildings/sky. Autocorrelation analysis confirm localized areas with similar feature values, while point-neighbor mapping identifies significant negative spatial correlations between greenery, buildings, and sky. The variograms illustrate maximum continuity ranges influenced by historical expansion processes, and shared continuity limit among all four categories. The uneven distribution of urban characteristics is evident in the heatmaps. The presented methodology can be adapted for similar analyses in diverse urban contexts, providing a valuable tool for urban researchers and planners.

Keywords:
green view index, spatial continuity, image segmentation, street view.

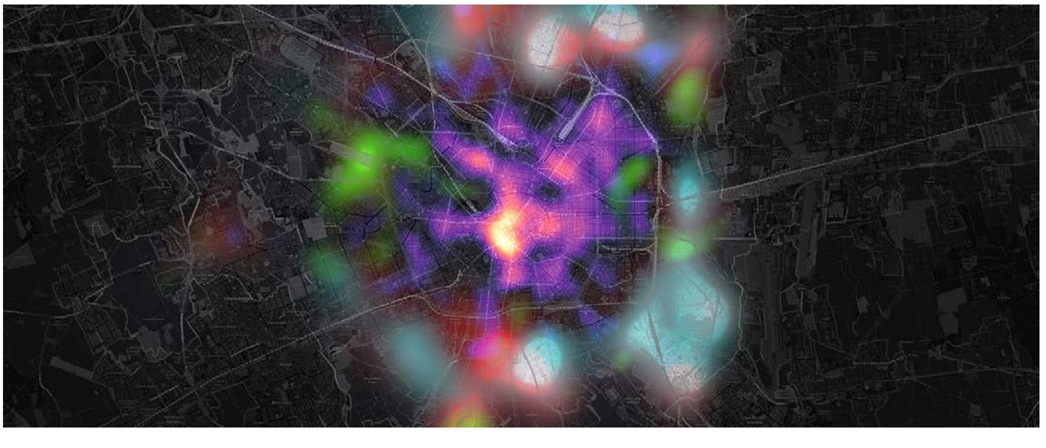

Heatmap of Milan.
Elaboration of the author.

doi.org/10.3280/oa-1180-c576

Introduction

To understand the perception of spaces, it is essential to consider various factors that influence views and experiences. Research has shown that green spaces' size, attractiveness, and appropriateness play a crucial role in shaping people's perceptions of restorative effects and accessibility of these areas [Kaplan and Kaplan 1989; Lee et al. 2017]. Additionally, accessibility and availability of green spaces correlate significantly with residents' perceptions of the quality of urban green spaces and their satisfaction [He et al. 2022]. Furthermore, personal perception of factors such as safety can be modified by the physical distance of green spaces, indicating the intricate relationship between perception and environmental factors [Lee et al. 2017].

In 2019, Yang proposed a method to calculate the Green View Index from perceived greenness in photographs taken on the street [Yang et al., 2009]. Initially based on computer vision techniques for chromatic analysis, the method has since been refined using image segmentation techniques [Li et al. 2015].

Measuring the green coverage of residential units, the visible greening of surrounding street space, and public green land around residential areas through indicators such as the green coverage index and green view index provides valuable information on the impact of green spaces on communities [Gu et al. 2019; Kumakoshi et al. 2020].

Furthermore, street view images and deep learning technology have allowed analysis of street space perception factors and their correlation with human activity, highlighting the relationship between environmental perceptions and human behavior [Stancato, Piga 2024; Tao et al. 2022].

Furthermore, the impact of street space perception factors on elderly health has been analyzed using street view images and deep learning technology, highlighting the role of street view, green space, and blue space in preventing depression in the elderly [Boffi et al. 2022; Meng et al. 2020]. Street view perception plays a crucial role in urban planner design and improvement of urban street layouts [Sun et al. 2023].

As is known, the first law of Tobler suggests that the closer the elements, the higher the mutual influence or relationship [Tobler 1970; Walker 2022]; living in the urban environment, this concept means that the psychological effects of the urban environment do not only depend on being exposed to one spot but also to the continuity of a condition [Nejasmic et al. 2015].

The visual quality of the urban environment can be affected by several spatial elements, such as consistency and continuity in visible elements [Ye et al. 2019]; mapping how the visual panorama changes across the city can help identify problematic streets, proposing appropriate zoning rules, and suggesting microscale design strategies.

This work describes an approach to visual feature mapping of the urban environment to measure and represent the proportion of natural and built elements visible at street level. In addition, this paper focuses on spatial continuity to highlight zones of homogeneous characteristics.

Materials and Methods

The focus of this work is the built environment of Milan (Italy) for its central role in the Multilayered Urban Sustainability Action (MUSA) project of the National Recovery and Resilience Plan (NRRP).

For generating the initial location of the street points, I used the street polyline shape file from the Geoportale of Milan [Comune di Milano 2023]. This file is an open-source representation of the street axis; in that representation, when a two-lane road is divided by a tree-lined median it is represented as two parallel lines, this representation is useful in considering the different perceptions on the two sides of the tree-lane.

QGIS 3.34.1 has been employed to manage the shapefiles and generate points and heatmaps. Google_ streetview 1.2.9 is a Python library for managing communication with the Google

API and downloading spherical views from various positions along streets worldwide. GluonCV 0.10.5: is an open-source deep learning library designed for computer vision tasks. It is built on top of Apache MXNet; it provides pre-trained models, tools, and utilities to facilitate the development and deployment of computer vision applications [Guo et al. 2020].
ADE20K developed by MIT, is a dataset commonly used for semantic segmentation tasks in computer vision. It includes images across various scenes and provides pixel-level annotations for objects and their categories.
Researchers and developers use ADE20K to train and evaluate algorithms for scene understanding [Zhou et al. 2017]. Geostatpsy 0.0.26 is a Python library related to geostatistics, which involves the analysis and interpretation of spatial data [Pyrcz 2022].
Random points have been generated from the Milan street network with a minimum distance of 100 meters to ensure a diffuse distribution throughout the city territory. Subsequently, georeferenced images were collected by querying the Google Street View™ API with the coordinates extracted from the shapefile.
The images provided by Google are reasonably close to the selected points, with a maximum deviation of 5 meters. Spatial continuity analysis involves the computation of variograms that examine the degree of variation in urban features across space; to ensure comparability, the spatial analysis process involves normalizing the recorded quantities of urban features to a standard scale. In this context, the "range" measure refers to the distance beyond which the spatial correlation between feature values becomes negligible.
Variogram maps illustrate how the correlation strength decreases with increasing separation distance. The maximum range and related continuity orientation (azimuth) have been calculated for each feature analyzed. The term "orientation" we will use in variogram analysis corresponds to the azimuthal direction in which spatial continuity is examined. It helps to understand whether the correlation between urban features is directionally dependent or isotropic. In summary, the analysis encompasses the evaluation of spatial patterns, the range that indicates the spatial extent of correlation, and the orientation that provides insight into the directional dependencies.
These variogram insights are crucial for understanding the distribution and relationships among urban features in the Milan street network. For evaluating possible overlapping of the analyzed feature, I built a matrix of feature/orientation considering the azimuth of the maximum range of each feature; the minimum distance value in the matrix of ranges is considered the limit of possible shared continuity among the analyzed features. Urban features are then represented as weighted heatmaps, informed using the panorama's coordinates provided by the related Google metadata.

Fig. 1. Spherical panorama view of one point in the street network of Milan. Source: Google Street View™.

Fig. 2. Image semantic segmentation of the panorama picture; colored masks highlight different features: in azure the sky, brown the buildings, green vegetation, blue cars, gray street, orange and yellow the barriers. Elaboration by the author.

Results

From the points generated onto the street network polylines, 3138 panorama pictures are obtained (fig. 1) and segmented according to the ADE20K urban categories (fig. 2).
Data related to vertical natural elements have been aggregated in an umbrella "greenery" category, horizontal natural elements have been aggregated as "ground".
Because all images are shot on streets, this kind of surface is common to all dataset and its quantity can be derived by subtracting other features from the scene.
For this reason, in the following analysis, the street feature is not considered, taking into account only features that can vary along the street section, such as the amount of greenery and buildings.
After normalizing the values of the four categories, we can compare how these are related; in particular, it is possible to triangulate the values of the greenery, buildings, and sky.
As shown in (fig. 3), the amount of visible sky is inversely proportional to the buildings; furthermore, we can see that increasing greenery is inversely proportional to both buildings and the sky.
These results suggest that these three elements are linearly concurrent in determining the articulation of the scene.

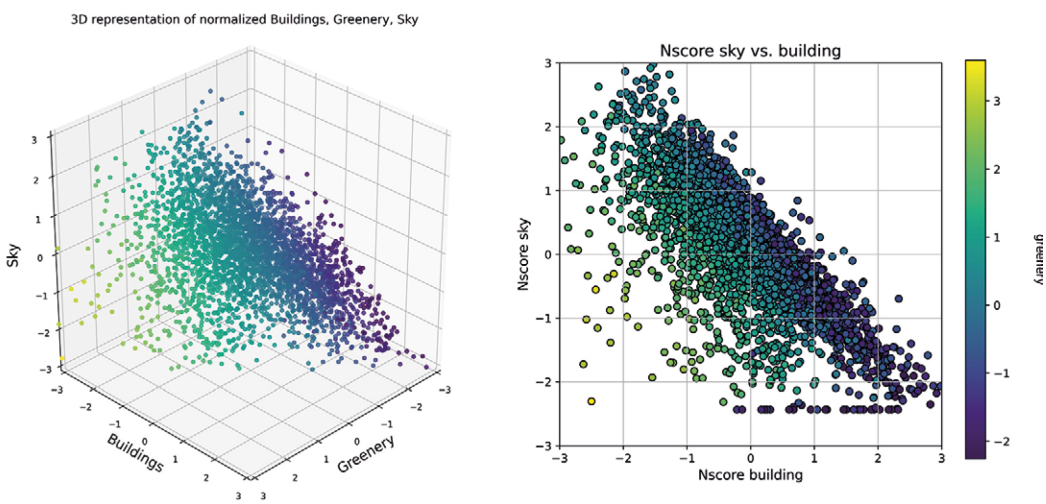

Fig. 3.On the left, three-dimensional scatter plot of urban features. On the right, planar scatterplot of the sky versus buildings feature. The gradient represents the amount of greenery in the two charts. The triangular shape of the point distribution shows how these three features are reciprocally concurrent. Elaboration by the author

Computing a Moran I analysis [Moura and Fonseca 2020] for autocorrelation (table 1) we can verify that all four features have positive results, meaning that points with a similar value of a feature tend to be close, then we can expect to see circumscribed areas of similar conditions. Autocorrelation can be deepen by analyzing the reciprocal spatial correlations of the four features using the Queen algorithm for point-neighbor mapping [Moura and Fonseca 2020] to inform an Ordinary Least Squares regression (OLS) analysis. Values in table 2 confirm significant negative spatial correlations between greenery, buildings, and sky variables. In addition, it does not reveal a significant relationship between ground values and buildings. The correlation between ground and sky indicates that the ground percentage increases the amount of visible sky. At the same time, the ground is also positively correlated with greenery. Taking this information together, we expect to see high-intensity areas of trees, ground, and sky that occupy opposite zones compared to the buildings; furthermore, we expect to see partial overlapping of greenery and ground, while greenery and sky should occupy different areas; in addition, ground and sky should overlap but in different zones compared to the one occupied by greenery.

Value→ Feature↓	Moran I	p sim
greenery	0.290	0.001
ground	0.244	0.001
building	0.497	0.001
sky	0.508	0.001

Table 1. Moran I spatial autocorrelation analysis. All features show positive significant ($p<0.05$) correlations, meaning that like values tend to cluster.

Feature	variable	coefficient	std_err	t_stat	p_val
greenery	*Ngroung*	0.1762	0.0144	12.2597	0.0000
	Nbuilding	-1.1450	0.0144	-79.2963	0.0000
	Nsky	-0.6705	0.0139	-48.0809	0.0000
ground	Nbuilding	0.0262	0.0304	0.8629	0.3883
	Ngreen	0.2597	0.0212	12.2597	0.0000
	Nsky	0.1944	0.0220	8.8204	0.0000
building	Nground	0.0091	0.0105	0.8629	0.3883
	Ngreen	-0.5828	0.0074	-79.2963	0.0000
	Nsky	-0.6169	0.0071	-86.7527	0.0000
sky	*Ngroung*	0.1246	0.0141	8.8204	0.0000
	Nbuilding	-1.1445	0.0132	-86.7527	0.0000
	Ngreen	-0.6332	0.0132	-48.0809	0.0000

Table 2. Ordinary Least Squares regression (OLS) analysis. Each feature is analyzed as a dependent variable on the other three in search of mutual influences. The red values represent the increasing effect, the blue values the decreasing effect, and green are significant statistics ($p<0.05$).

The variograms of the four categories (fig. 5) show an anisotropic reality where maximum continuity ranges and orientation (azimuths) are the following: greenery 2.5 Km at 45° N; building 4.2 Km at 45° N; ground 7.0 Km at 67.5° N; sky 4.9 Km at 90°N (fig. 4).
These results suggest that significant visual continuity in terms of feature proportions follows mainly a diagonal trend, stretching from the southwest to the northeast. The ground feature is the only one that presents an isotropic distribution, slightly prolonged in one direction.

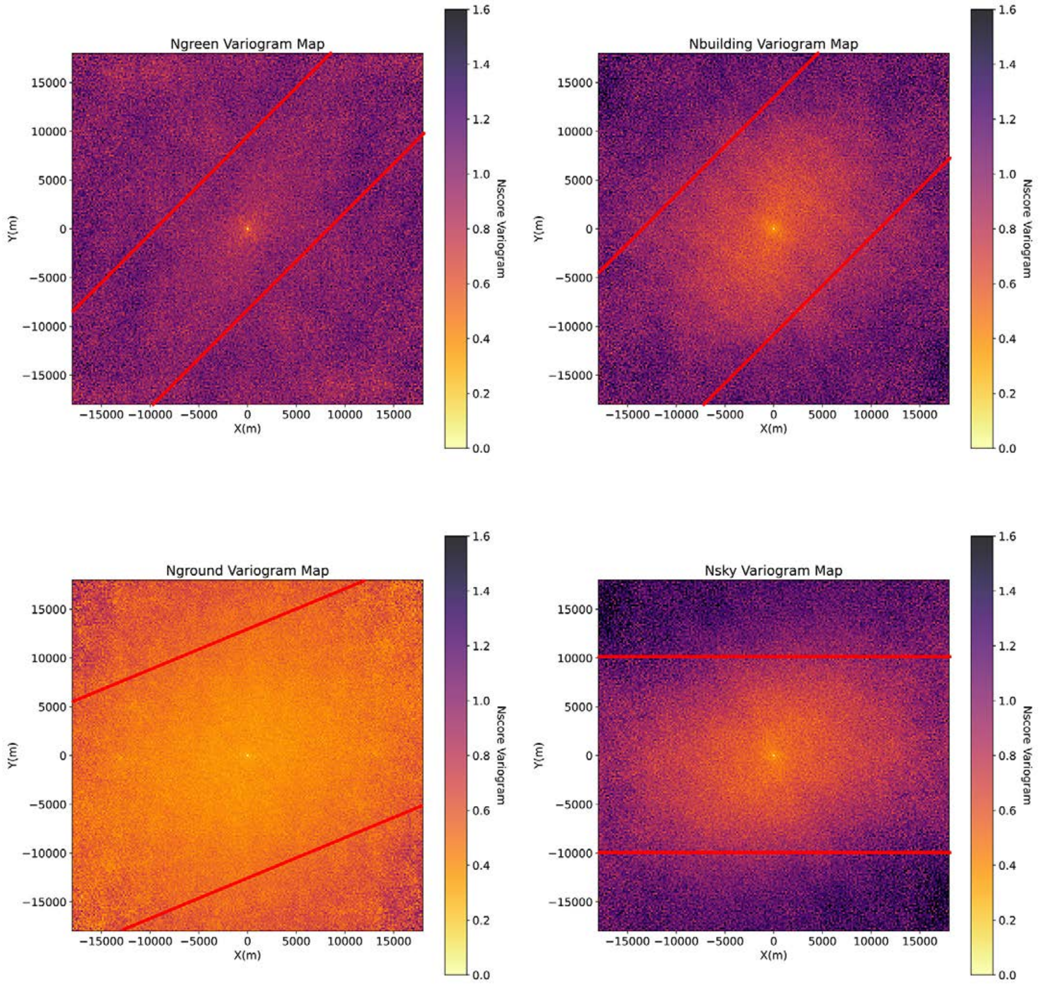

Fig. 4. Variograms maps showing the anisotropic nature of the data. On top left, greenery; top right, buildings; bottom left, ground; bottom right, sky. The plasma gradient highlights the distribution of positive correlations; red lines mark the azimuth of maximum spatial continuity, namely: greenery 45°; building 45°; ground 67.5°; sky 90 °.
Elaboration by the author.

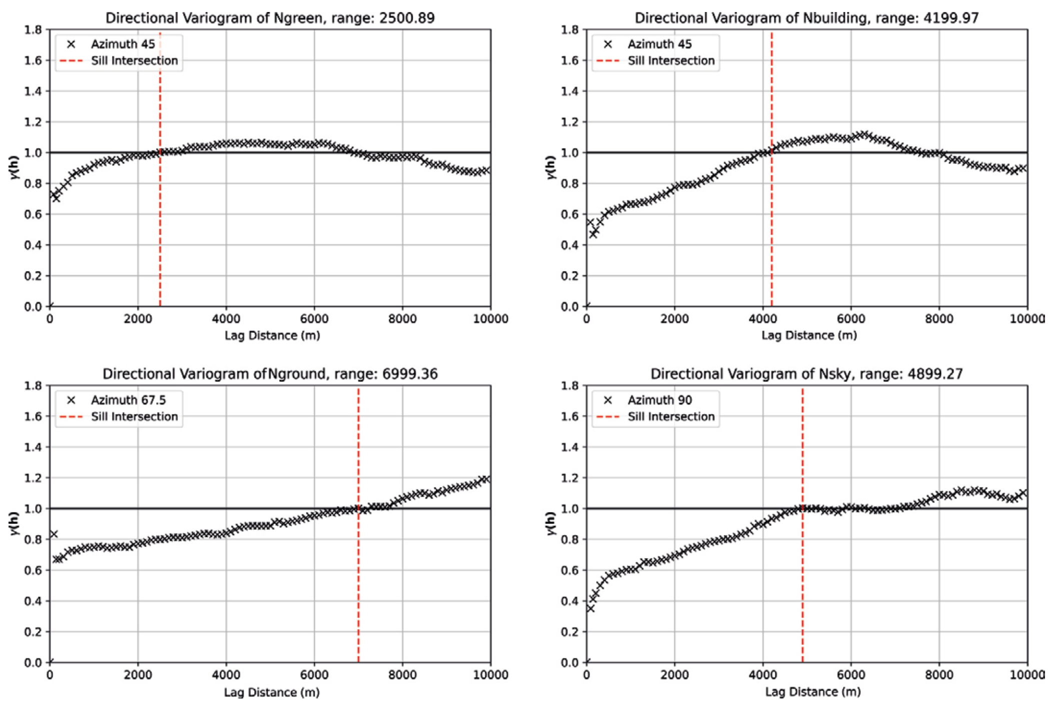

Fig. 5. Maximum range variograms of the four features: on the top left, greenery; top right, buildings; bottom left, ground; bottom right, sky. The bold black line is the sill, where correlation become negligible.
The red dashed line represents the point where data cross the sill and marks the maximum continuity range in a direction. Elaboration by the author.

Moreover, among these ranges, the the maximum greenery value result is 2.5 Km; however, this cannot be considered the shared continuity range when the four categories are evaluated together. Comparing the ranges of all categories at the three azimuth angles (45°, 67.5°, 90°), we can assess that the limit of possible continuity in all four categories together is 1.9 Km (table 3).

Table 3. Spatial continuity ranges for the four urban features. The three azimuth angles relate to the maximum ranges of the four features as shown in Fig. 5, and Fig. 4. In green, the maximum range for greenery; in red, the largest range for the urban features at the three angles, and in blue, the smallest range.

Azimuth→ Feature↓	45°	67.5°	90°
greenery	2500	2201	1900
ground	6799	6999	6399
building	4200	4099	4100
sky	4199	4800	4900

This limit approximatively corresponds to the average distance between Milan's urban expansion boundaries. The proportion of urban characteristics is not evenly distributed in the city texture due to its historical expansion process; for instance, the green elements directly visible at street level are mainly distributed out of the Beruto urban plan boundary (1889) except for large green areas such as Sempione Park. The ground feature, representing horizontal natural areas, is more intense where the street sections are more prominent, as in Enrico Fermi Street in the northwest. The proportion of visible sky is affected by all vertical elements, both natural and built; for this reason, the larger sky proportions are localized to highways in the southeast. The remaining feature of the building is denser in the city center inside the Beruto expansion ring.

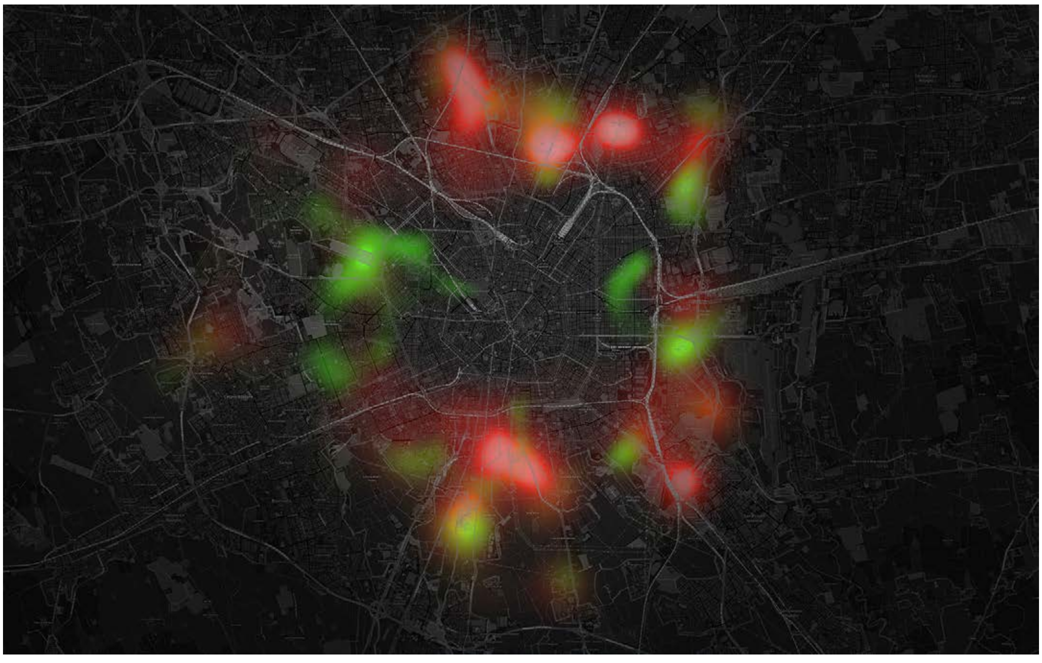

Fig. 6 Heatmap of greenery (in green) and ground (in red) overlapped. Elaboration by the author.

Fig. 7. Heatmap of buildings (magma gradient) and sky (azure) overlapped. Elaboration by the author.

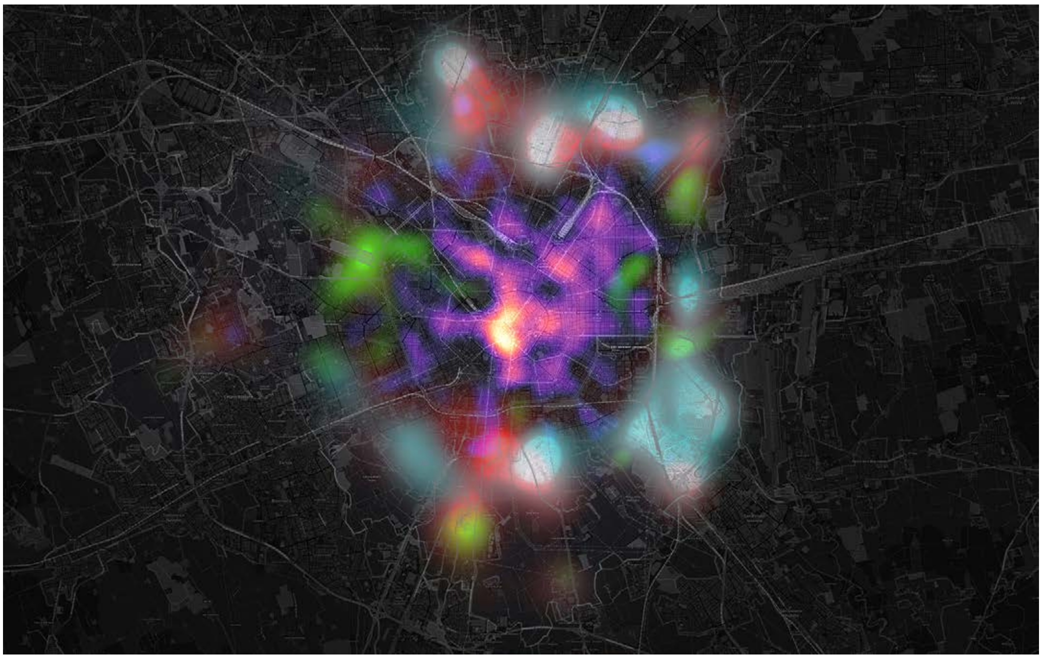

Fig. 8. Heatmap of all four features overlapped. Elaboration by the author.

To compare where the four features are more intense, I generated four heatmaps weighted with the features of the point.
Combining the greenery with the ground heatmap (fig. 6), and the buildings with the sky heatmap (fig. 7), it is possible to observe how the natural elements are distributed mainly on a ring surrounding the city center, where, on the contrary, the buildings are denser.
This result is not surprising, but remarkably, the two halves of the town show different uses of natural elements. Although the west side shows more vertical vegetation,

the east side has a larger proportion of visible horizontal natural elements. Moreover, larger sky proportions are visible where the ground feature substitutes both buildings and trees on the east side of the modern expansion ring. In (fig. 8) the four heatmaps are overlapped to represent the constellation of street view features in the entire town.

Discussion

The present study systematically analyzed spatial patterns and correlations between various urban characteristics within the Milan street network. The methodology involved generating random points throughout the city, ensuring a diffuse distribution, followed by querying the Google Street ViewTM API to obtain images in the selected points. Spatial continuity analysis, represented through variograms, provided valuable information on the variation of urban features across space. The "range" parameter indicated the spatial extent of the correlation, whereas the orientation parameter revealed directional dependencies. The results suggest that the distribution of urban features is not uniform, and understanding these patterns is crucial to grasping the visual dynamics within the Milan street network.
Moving to the results, the segmentation of panorama pictures based on ADE20K urban categories yielded 3138 images, and after normalizing the values, the triangulation of the greenery, buildings, and sky indicated inverse proportional relationships. Moran I analysis confirmed a positive autocorrelation for all four features, indicating localized areas with similar feature values. The ordinary least squares regression (OLS) revealed significant negative spatial correlations between greenery, buildings, and sky, while ground values do not show a significant relationship with buildings.
Variograms of the four categories illustrated maximum continuity ranges, with major visual continuity following a diagonal trend from the southwest to the northeast. The analysis suggested that the limit of possible continuity for all four categories is approximately 1.9 Km. Furthermore, the uneven distribution of urban characteristics in the texture of the city, influenced by historical expansion processes, was evident in the heatmaps. In conclusion, the study provides a comprehensive understanding of the spatial distribution and correlations between urban characteristics in the Milan street network. The findings contribute to urban planning and design by highlighting areas of concentrated features and informing decisions on green spaces, buildings, and sky visibility. The methodological approach presented here can be adapted to similar analyses in other urban contexts, offering a valuable tool for urban researchers and planners.

Limitations

In future work, it will be helpful to apply the method to a denser dataset to describe the urban features across the city with a finer grain. Further research could inquire about the axial continuity of these features in Milan and relate them with the history of urban expansion.

Acknowledgment
This research has been developed within the MUSA – Multilayered Urban Sustainability Action – project, funded by the European Union – NextGenerationEU, under the National Recovery and Resilience Plan (NRRP) Mission 4 Component 2 Investment Line 1.5: Strengthening of research structures and creation of R&D "innovation ecosystems", set up of "territorial leaders in R&D".

References

Boffi M., et al. (2022). Visual post-occupancy evaluation of a restorative garden using virtual reality photography: Restoration, emotions, and behavior in older and younger people. In *Frontiers in Psychology*, n. 13. <https://www.frontiersin.org/articles/10.3389/fpsyg.2022.927688>

Comune di Milano. (2023). Open data | Geoportale SIT. Retrieved 1 November 2023 <https://geoportale.comune.milano.it/sit/open-data>

Gu W., Chen Y., Dai M. (2019). Measuring Community Greening Merging Multi-Source GeoData. In *Sustainability*, vol. 11, n. 4. <https://doi.org/10.3390/su11041104>

Guo J., et al. (2020). GluonCV and GluonNLP: Deep Learning in Computer Vision and Natural Language Processing. In *Journal of Machine Learning Research*, n. 21, pp. 1–7.

He S., et al. (2022). Resident Satisfaction of Urban Green Spaces through the Lens of Landsenses Ecology. In I*nternational Journal of Environmental Research and Public Health*, vol. 19, n. 22, pp. 1-15.

Kaplan R., Kaplan S. (1989). *The experience of nature: A psychological perspective*. New York: Cambridge University Press.

Kumakoshi Y., et al. (2020). Standardized Green View Index and Quantification of Different Metrics of Urban Green Vegetation. In *Sustainability*, vol. 12, n. 18. <https://doi.org/10.3390/su12187434>

Lee Y., Gu,N., An S. (2017). Residents' perception and use of green space: Results from a mixed method study in a deprived neighbourhood in Korea. In *Indoor and Built Environment*, vol. 26, n. 6, pp. 855–871. <https://doi.org/10.1177/1420326X16661024>

Li X., et al. (2015). Assessing street-level urban greenery using Google Street View and a modified green view index. In *Urban Forestry & Urban Greening*, vol. 14, n. 3, pp. 675–685. <https://doi.org/10.1016/j.ufug.2015.06.006>

Meng L., et al.(2020). The Impact of Street Space Perception Factors on Elderly Health in High-Density Cities in Macau – Analysis Based on Street View Images and Deep Learning Technology. In *Sustainability*, vol. 12, n. 5 <https://doi.org/10.3390/su12051799>

Moura A. C. M., Fonseca B. M. (2020). ESDA (Exploratory Spatial Data Analysis) of Vegetation Cover in Urban Areas – Recognition of Vulnerabilities for the Management of Resources in Urban Green Infrastructure. In *Sustainability*, vol. 12, n. 5. <https://doi.org/10.3390/su12051933>

Nejasmic J., Bucher L., Knauff M. (2015). The construction of spatial mental models – A new view on the continuity effect. In *Quarterly Journal of Experimental Psychology*, vol. 68, n. 9, pp. 1794–1812. <https://doi.org/10.1080/17470218.2014.991335>

Pyrcz M. (2022). geostatspy: Geostatistical methods from GSLIB: Geostatistical Library translated and reimplemented in Python [Python, OS Independent]. <https://github.com/GeostatsGuy/GeostatsPy>

Stancato G., Piga B. E. A. (2024). Image Segmentation and Emotional Analysis of Virtual and Augmented Reality Urban Scenes. In A. Giordano, M. Russo, R. Spallone (Eds.). *Beyond Digital Representation: Advanced Experiences in AR and AI for Cultural Heritage and Innovative Design*, pp. 443–458. <https://doi.org/10.1007/978-3-031-36155-5_28>

Sun J., Zhang Y., Yang X. (2023). A suggestion method for urban perception improvement using street-view images. In *Second International Symposium on Computer Applications and Information Systems (ISCAIS 2023)*, 24-26 March, Chengdu, China, pp. 386-392., pp. 386–392. <https://doi.org/10.1117/12.2683558>

Tao Y., et al. (2022). Measuring the Correlation between Human Activity Density and Streetscape Perceptions: An Analysis Based on Baidu Street View Images in Zhengzhou, China. In *Land*, vol. 11, n. 3 <https://doi.org/10.3390/land11030400>

Tobler, W. R. (1970). A Computer Movie Simulating Urban Growth in the Detroit Region. In *Economic Geography*, n. 46, pp. 234–240. <https://doi.org/10.2307/143141>

Walker, R. T. (2022). Geography, Von Thünen, and Tobler's First Law: Tracing the Evolution of a Concept. In *Geographical Review*, vol. 112, n. 4, pp. 591–607. <https://doi.org/10.1080/00167428.2021.1906670>

Yang J., et al. (2009). Can you see green? Assessing the visibility of urban forests in cities. In *Landscape and Urban Planning*, vol. 91, n. 2, pp. 97–104. <https://doi.org/10.1016/j.landurbplan.2008.12.004>

Ye Y., et al. (2019). The visual quality of streets: A human-centred continuous measurement based on machine learning algorithms and street view images. In *Environment and Planning B: Urban Analytics and City Science*, vol. 46, n. 8, pp. 1439–1457. <https://doi.org/10.1177/2399808319828734>

ZhouIn B., et al. (2017). Scene Parsing through ADE20K Dataset. In *2017 IEEE Conference on Computer Vision and Pattern Recognition (CVPR)*, 21-26 July 2017, Honolulu, Hawaii, pp. 5122–5130. <https://doi.org/10.1109/CVPR.2017.544>

Author
Gabriele Stancato, Politecnico di Milano, gabriele.stancato@polimi.it

To cite this chapter: Gabriele Stancato (2024). TQuantifying city dynamics: exploring urban representation in Milan's street features. In Bergamo F., Calandriello A., Ciammaichella M., Friso I., Gay F., Liva G., Monteleone C. (Eds). *Misura / Dismisura. Atti del 45° Convegno Internazionale dei Docenti delle Discipline della Rappresentazione/Measure / Out of Measure. Transitions. Proceedings of the 45th International Conference of Representation Disciplines Teachers.* Milano: FrancoAngeli, pp. 2091-2102.

 Isbn 9788835166948